JOURNAL OF SOLID STATE CHEMISTRY 7, 454–460 (1973)

Pseudophase Behavior in the Epsilon and Iota Regions of the Praseodymium Oxide–Oxygen System

R. P. TURCOTTE, M. S. JENKINS, AND L. EYRING

Batelle Northwest Laboratories, Richland, Washington 99352 and Pilkington Bros., Ltd., Lancashire, United Kingdom and Arizona State University, Tempe, Arizona 85281

Received November 10, 1972

Besides line and nonstoichiometric phases complex oxide systems exhibit reproducible bivariant behavior, termed pseudophases, in the two-phase regions. This occurrence exaggerates chemical hysteresis. Two of these pseudophases in the praseodymium oxide–oxygen system are examined in some detail by tensimetric and high temperature X-ray studies.

The tensimetric measurements show marked and progressive shifting of the curves away from stoichiometry with increasing pressure. In addition, unusual reversals are seen to occur both in oxidation and reduction. X-ray diffraction patterns at temperature are seen to show systematic changes in line positions and line widths. These are analyzed and their implications discussed in terms of suggested structural changes. Similarities and relevance to other systems are suggested.

Introduction

A phenomenological description of a system in the solid state which pretends to be exhaustive must distinguish a wide variety of behavior. For example there are phases near simple stoichiometric composition with only very slight compositional variation with temperature such as $ThO_{2-\delta}$ (*1*, *2*) or phases of very narrow width with more complicated stoichiometry such as the homologous series Ti_nO_{2n-1} (*3*). In addition there are phases which have an easily measurable but small range of composition as in the system Pr_nO_{2n-2} (*4*). In the present context such phases which may also exhibit polymorphism are called line phases.

One must add to these nonstoichiometric phases having reversible bivariant character over a wide range of composition. The most studied of these include UO_x ($2.0 \leq x \leq 2.25$), FeO_x ($1.05 \leq x \leq 1.19$), TiO_x ($0.7 \leq x \leq 1.25$) and PrO_x ($1.50 \leq x \leq 1.69$ and $1.72 \leq x \leq 2.00$). Various observers have described these as microheterogeneous, having microdomains, being microphasic, being coherently intergrown, etc., which implies that structurally they possess texture above the unit cell level. Subtle discontinuities in thermodynamic and structural behavior have suggested that these wide regions must be divided into areas having more coherent properties. For example, the FeO_x ($1.05 \leq x \leq 1.25$) phase has been described to have at least three distinct regions (*5*, *6*) and PrO_x ($1.71 \leq x \leq 2.00$) at least four (*7*).

In any system having more than one phase there must be a two-phase region separating each pair. These transitional regions are themselves being observed to be extremely complex showing marked premonitory behavior (*8*), hysteresis (*4*, *9*), and pseudophase formation (*4*).

Pseudophases in the present usage are reproducible and bivariant in *p*, *T*, *x* studies as a system transforms from one phase to another in one direction. The degree of pseudophase formation varies depending upon the direction of reaction, being more pronounced in going from less to more ordered regions among phases which may intergrow coherently. They may, however, be observed on either compositional side of a stoichiometric phase and hysteresis is augmented by this behavior.

An important recent review (*10*) of structural and compositional changes in the TiO_x system ($1.75 \leq x \leq 1.98$) relates an hourglass shaped hysteresis curve over the compositional interval

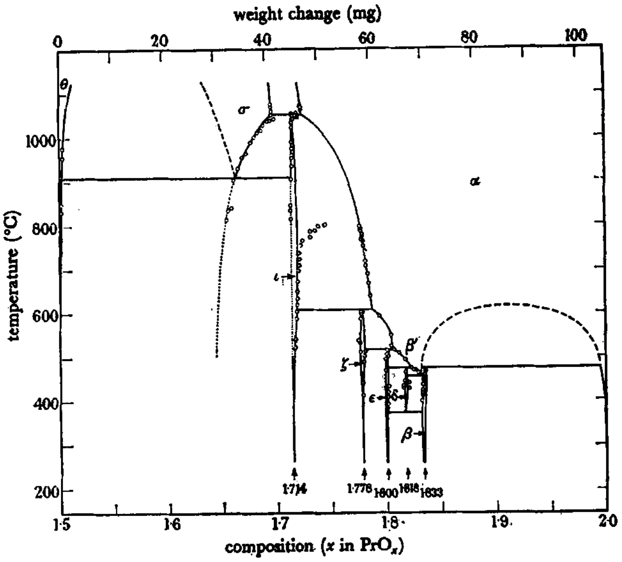

FIG. 1. Phase relations in the praseodymium oxide system.

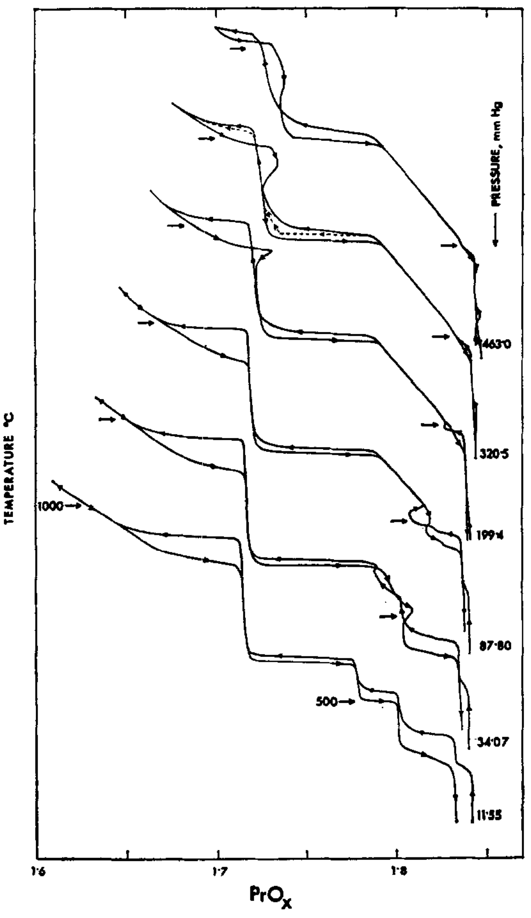

FIG. 2. Representative isobars in the praseodymium oxide system.

to crystallographic shear (CS) structures utilizing (121) planes in the parent rutile in the region $1.75 \leqslant x \leqslant 1.90$ where the first large loop occurs and (132) CS structures in the other large loop ($1.93 \leqslant x \leqslant 1.98$). Between these branches the loop collapses and is almost reversible correlating with a region of oxides whose structures are characterized by the "swinging" of shear planes between (121) and (132).

We shall focus here on a particular manifestation of pseudophase behavior on the oxygen-rich side of the ι and ε phases of the praseodymium oxide–oxygen system. These phases are members of a homologous series apparently structurally related by some principle other than crystallographic shear. The phase diagram including the regions of our interest is shown in Fig. 1 (*4*). The behavior we wish to examine more closely is illustrated by the isobaric curves at 463.0 and 34.07 Torr in the ι and ε region of Fig. 2 (*11*). The sequential development of the isobars with increasing pressure shows the vertical portions of the curves to shift significantly to higher compositions than expected if the intermediate phases are highly ordered and nearly stoichiometric. As the hysteresis curves shift they are also observed to become less steep and to develop a crossover in that region.

Experimental Part

Hyperstoichiometric pseudophase formation of the type being considered is marked in the

PrO_x-O_2 system where the highly symmetric nonstoichiometric α phase is stable in the temperature and pressure region of the ordered intermediate phases. Where this condition is not met [i.e., in the TbO_x-O_2 (*11*, *12*) and the CmO_x-O_2 (*13*, *14*) systems] this phenomenon is not encountered. For purposes of this discussion the location of the pseudophase in the phase field is indicated by two Greek letters written together. For example, the symbol αι refers to a bivariant phase at the interface between the α and ι phases. As will be further discussed, the α and ι microcomponents of αι are independently observable by X-ray diffraction methods existing in unchanging proportions over large temperature ranges.

All experiments were carried out using 99.999% PrO_x supplied by the Lindsay Division of the American Potash and Chemical Corporation. The tensimetric studies were made using an Ainsworth balance possessing automatic temperature and pressure control with an eight gram sample suspended in an alumina bucket by a platinum wire (*6*). X-ray studies were accomplished by means of a Philips high temperature diffractometer (*15*) and a high temperature Nonius Guinier–Lenné camera (*16*). Temperatures were measured in all cases with Pt–Pt/10% Rh thermocouples calibrated as required. Thoria was used as an internal standard in the X-ray patterns and all data were reduced by computer methods [$\lambda(K\alpha 1) = 1.54051$].

Results and Discussion

Thermogravimetric Analysis

Isobaric thermogravimetric experiments as displayed by representative curves in Fig. 3 were performed at a rate of temperature increase of 0.5°C per minute. They portray graphically the transformation of $PrO_{1.833}$ (β phase) to $PrO_{1.800}$ (ε) to PrO_x (α) and return. The δ phase ($PrO_{1.818}$) is observed to be complicating the reaction to some degree. It is important to realize that the observed behavior is reproducible in all the regions discussed. A shift to higher composition with increasing pressure is marked as is the narrowing of the temperature range of the reaction.

Similar isobaric runs in the $PrO_{1.714}$ (ι) region have been made with great care and behavior similar to that shown in the two highest pressure curves in Fig. 2 is confirmed. Even upon sustaining conditions for one month there was no tendency for conversion to stoichiometric ι. In fact the unique ι line phase is not attained until the pressure is reduced to about 10 Torr.

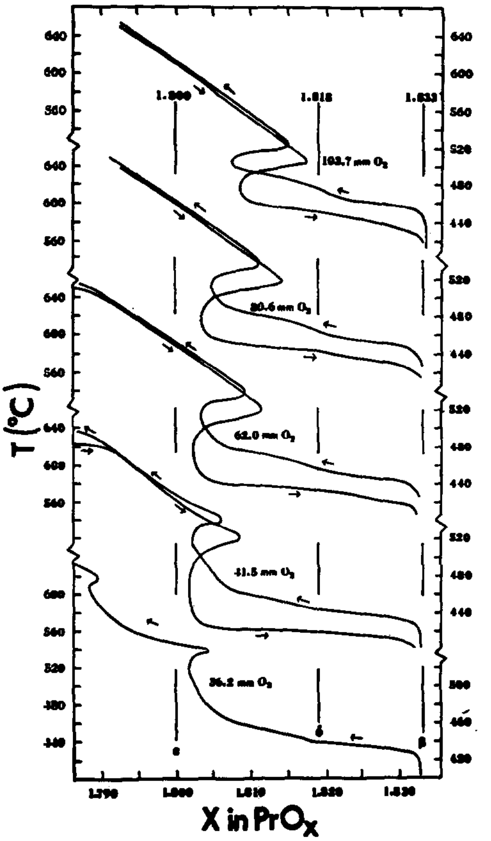

FIG. 3. Isobaric curves in oxidation and reduction between beta and alpha phases in the PrO_x–O_2 system.

In order to observe the transit from the oxygen excess αι pseudophase to stoichiometric composition (ι) isotherms of the following type were performed. At 843°C and 676 Torr the specimen is in the low-temperature region of the pseudophase (αι) with a composition of $PrO_{1.753}$. When the pressure was reduced to 6.8 Torr at constant temperature the oxide reduced to $PrO_{1.714}$. When the pressure was restored to 676 Torr, the composition increased only to $PrO_{1.721}$ indicating at this pressure a narrow compositional variation of ι phase at 843°C, the irreversible nature of the change and the metastability of the pseudophase.

In similar experiments at 32.79 Torr and 569°C, the ζ phase indicated a composition of $PrO_{1.789}$ based on the assumption that at a pressure of 6.46 Torr the composition was $PrO_{1.778}$. When the pressure was restored the composition increased only to $PrO_{1.780}$ giving a phase variation for ζ of 0.002 in oxygen to praseodymium ratio compared to 0.007 for ι phase and similar experiments in the ε region gave a compositional increase of 0.004 between 10 and 138 Torr.

X-Ray Analysis

The epsilon region pseudophase. Diffraction patterns obtained at temperature for the β, δ, ε, ζ and ι phases shown in Fig. 4 confirm those obtained earlier on samples quenched after long anneals (*17*) except for the ζ phase which appears to be polymorphic.

The diffraction patterns of samples maintained at O_2 pressures near two of the isobars of Fig. 3 (41 and 102 Torr) and filmed at a heating rate of 5°C/hr are shown in Figs. 5 and 6. The symbol α is used when general reference to the nonstoichiometric phase is intended. The symbol α^* is used to indicate probable short-range order characterized by regularly increasing line widths as the Bragg angle increases and α^{**} indicates the nonstoichiometric phase which shows a slight distortion from cubic symetry as evidenced by a diffraction pattern having $\beta_{111} > \beta_{200} < \beta_{220}$ (β_{111} = line width of the (111) reflection, etc.). Very weak superstructure lines also appear in

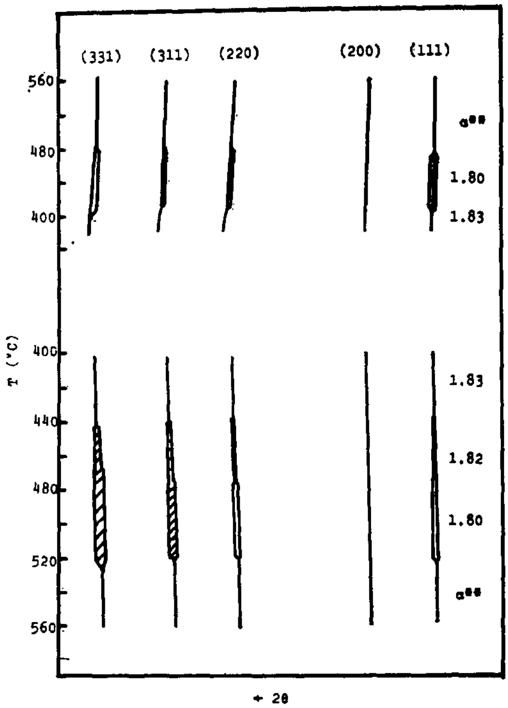

FIG. 5. Continuous high temperature diffraction patterns in the epsilon alpha region. 41 Torr O_2 with decreasing t (top) and increasing t (bottom).

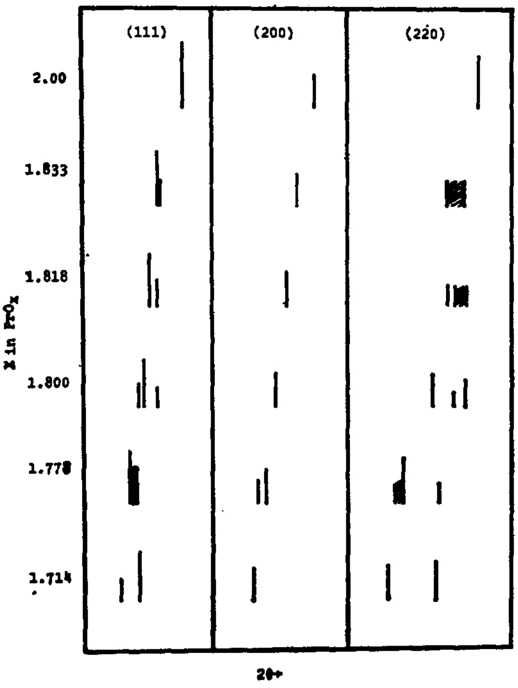

FIG. 4. Main reflections of ordered phases in the PrO_x–O_2 system obtained at equilibrium conditions of temperature and pressure.

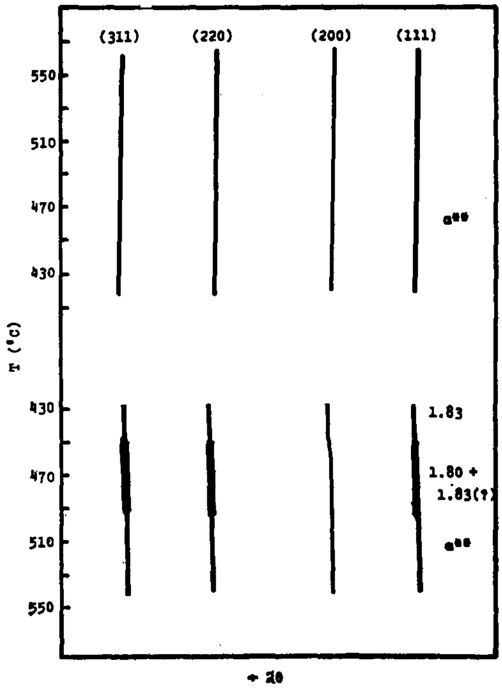

FIG. 6. Continuous high temperature diffraction patterns in the epsilon region. 102 Torr O_2 for decreasing t (top) and increasing t (bottom).

the α^{**} pattern. Transitions between α, α^*, and α^{**} appear to be continuous in passing from high to low temperature.

At 41 Torr the transformations seen in cooling are

$$\alpha \xrightarrow{475°\mathrm{C}} \varepsilon \xrightarrow{410°\mathrm{C}} \beta$$

while in heating the sequence is

$$\beta \xrightarrow{440°\mathrm{C}} \delta \xrightarrow{475°\mathrm{C}} \varepsilon \xrightarrow{520°\mathrm{C}} \alpha^{**}.$$

Agreement with the thermograms (Fig. 3) is particularly good with increasing temperatures. With decreasing temperature the apparent $\alpha^{**} \rightarrow \varepsilon$ break temperature is significantly lower than expected from the thermogram, a trend which increases with increasing pressure so that by 102 Torr (Fig. 6), no significant line splitting is observed at all on the cooling cycle, although there are correlations relative to changes in lattice parameter.

Since the line splittings in these patterns are so slight, the reflections may be conveniently indexed on the basis of a pseudocubic (fluorite) unit cell. The lattice parameters so obtained in an isobaric set, vary in a fashion directly comparable to the tensimetric behavior as shown in Fig. 7 for several O_2 pressures. At 102 mm O_2 one may observe the contraction of the lattice as the temperature is decreased from 540°C. At 500°C (see Fig. 3) the sample is reduced from $PrO_{1.817}$ to about $PrO_{1.808}$ at 470°C as shown by the curve reversal. The compositional change is reflected in the X-ray data by a decrease in the rate of change of the lattice parameter with temperature since in this case the thermal and compositional effects are in opposition. The transition to β at 460°C on the other hand shows an increased $\Delta a/\Delta T$ since the sample oxidation and decreasing temperature both cause a decrease in the lattice parameter. Analogous behavior is seen at lower pressures as shown.

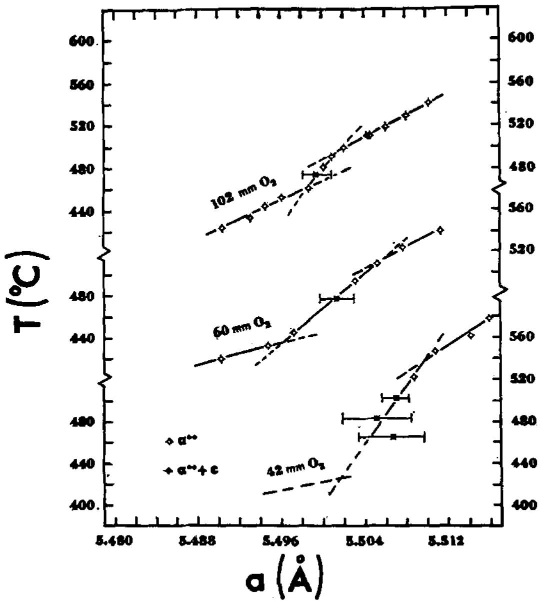

FIG. 7. Lattice parameter of the fluorite pseudocell in the epsilon region as a function of temperature and pressure.

The iota region pseudophase. The tensimetric isobaric studies (*4*, *11*) demonstrate a well developed pseudophase behavior in the $\alpha\iota$ region at pressures in excess of 150 Torr. High-temperature diffractometer measurements were made at several pressures in this region. The profile for the 220 reflection at 635 Torr is shown as representative of these in Fig. 8. The 220 peak which is single for α is split equally for ι. The superimposed peaks illustrated in Fig. 8 were analyzed on a curve resolver. A single phase α peak is shown at 779°C. At 881°C conversion to ι is about 50% complete. As the temperature is increased the α peak is seen to move to lower 2θ values within the envelope of ι as it weakens and disappears. This movement results from the rapid decrease in composition with the concomitant increase in lattice parameter as the temperature increases while the positions of the reflections in the ι phase remain virtually unchanged. Sigma phase exists alone at 1133°C.

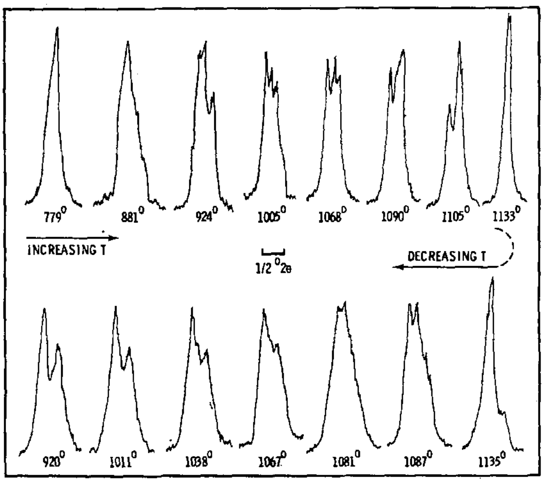

FIG. 8. (220) Reflections in the iota pseudophase region at 635 mm O_2.

At 1087°C, in cooling, the peak was split evenly with a separation of 0.10° at 2θ. It is believed that the low angle peak is α while the other is the $(\bar{2}20)$ reflection of ι. The $\sigma \rightarrow \alpha$ conversion presumed to have occurred between 1135 and 1087°C was not apparent, probably because the peak separation for the narrow miscibility gap is so small (0.001 Å in the lattice parameter). As the temperature was further reduced the reverse movement of the α peak in the ι envelope was followed. At 920°C the superposition of the α peak and the ι $(\bar{2}20)$ is apparent, suggesting a composition in excess of $PrO_{1.721}$.

In general, the X-ray results agree well with the interpretations of the tensimetric work but there are some anomalies in apparent relative phase concentrations as between the X-ray and gravimetric work. For example the gravimetric curves indicate about 50% α phase on cooling for some isobars but only 10% is apparent by X-ray diffraction. In other cases quantitative agreement is obtained and a clear explanation for the differences is not available.

Conclusions

It is apparent from these observations that there exist many superficial similarities in behavior in the $\alpha\iota$ pseudophase regions when observed by means of tensimetric and X-ray measurements, however, there are marked differences in detail and these differences depend to some extent on temperature and pressure since these govern the stability of neighboring phases.

On the high composition side of $PrO_{1.800}$, quite different "structures" are indicated in heating or cooling cycles and furthermore there are marked structural differences in comparing cooling runs at different pressures. With heating, the pseudophase behavior is a result of incomplete order → order transformations whereas with cooling (at 41 Torr) it is a result of an incomplete disorder → order change. On cooling cycles at pressures of 60 Torr and higher there is no evidence for the triclinic cell typical of stoichiometric $PrO_{1.800}$. Rather, broadening of certain reflections corresponding to the line splitting observed for $PrO_{1.800}$ but to lesser degree and the appearance of weak superstructure lines suggest a condition of partial order for $\alpha\varepsilon$ relative to the pure ε composition.

The following model of pseudophase formation in the ε region is suggested. Order → order transformations become progressively less complete with increasing pressure and temperature. Microdomains of the starting and product material intergrow to give a metastable phase capable of developing long range order. In the cooling cycle there is an increasing order as $\alpha^* \rightarrow \alpha^{**} \rightarrow \varepsilon$ pseudophase. Having long range order in a broadly nonstoichiometric α phase is not unlike that in the σ phase ($1.5 \leqslant x \leqslant 1.69$) which has sharp superstructure lines characteristic of C-type $PrO_{1.5}$ even when the composition is $PrO_{1.69}$.

At the higher O_2 pressures and temperatures where the $\alpha\iota$ pseudophase may be observed, similar changes occur. In this case, however, the reaction is $\alpha \rightarrow \alpha\iota$ whether with cooling from higher temperatures or heating from lower. Consequently the X-ray diffraction behavior for $\alpha\iota$ is not greatly different in comparing heating and cooling cycles, in contrast to the ε region results.

There are some similarities to behavior in other oxide systems. Willis (*18*) has shown by neutron diffraction that there are defect clusters in UO_{2-x} which, although disordered at low concentration produce the U_4O_9 phase when they reach a higher concentration and are fully ordered and Belbeoch et al. (*19*), have shown that U_4O_9 itself exists in varying degrees of order. Structural studies of Roth (*20*), Manenc (*21*), and Koch and Cohen (*22*) on the Wüstite phase have led to a description of the $Fe_{1-x}O$ as composed of defect clusters of more or less order at high temperatures. The domains grow with cooling and are periodically spaced at room temperature.

This phenomenological description of phase reactions and transitions in coherently intergrown systems is the beginning of understanding fluorite related materials having extended defects.

Acknowledgments

It is a pleasure to express appreciation to the United States Atomic Energy Commission for support of this work.

References

1. R. J. Ackermann, E. G. Rauh, R. J. Thorn, and M. C. Cannon, *J. Phys. Chem.* **67**, 762 (1963).

2. J. S. Anderson *in* "High Temperature Technology," p. 285. Butterworths, Washington (1964).

3. S. Andersson, B. Collén, U. Kuylenstierna, and A. Magnéli, *Acta Chem. Scand.* **11**, 1641 (1957).
4. B. G. Hyde, D. J. M. Bevan, and L. Eyring, *Proc. Roy. Soc.* **259**, 583 (1966).
5. P. Vallet and P. Raccah, *C. R. Acad. Sci. Paris* **258**, 3679 (1964).
6. B. E. F. Fender and F. D. Riley, *J. Phys. Chem. Solids* **30**, 793 (1969).
7. M. S. Jenkins, R. P. Turcotte, and L. Eyring, "Chemistry of Extended Defects in Non-Metallic Solids" (L. Eyring and M. O'Keeffe, Eds.). North-Holland Publishing Co., Amsterdam (1970).
8. A. R. Ubbelohde, *J. Chim. Phys.* **33** (1966).
9. P. A. Faeth and A. F. Clifford, *J. Phys. Chem.* **67**, 1453 (1963).
10. L. A. Bursill and B. G. Hyde, "Progress in Solid State Chemistry" (Reiss and McCaldin, Eds.), Vol. 7, p. 177. Pergamon Press, Oxford (1972).
11. J. Kordis and L. Eyring, *J. Phys. Chem.* **72**, 2044 (1968).
12. B. G. Hyde and L. Eyring, "Rare Earth Research, III," (L. Eyring, Ed.), p. 623. Gordon and Breach, New York (1965).
13. T. D. Chikalla and L. Eyring, *J. Inorg. Nucl. Chem.* **31**, 85 (1969).
14. R. P. Turcotte, T. D. Chikalla, and L. Eyring, *J. Inorg. Nucl. Chem.*, in press (1972).
15. A. D. Burnham and L. Eyring, *J. Phys. Chem.* **72**, 4415 (1968).
16. R. P. Turcotte and L. Eyring, *J. Solid State Chem.* **3**, 265–272 (1971).
17. J. O. Sawyer, B. G. Hyde, and L. Eyring, *Bull. Soc. Chim. France*, 1190 (1965).
18. B. T. M. Willis, *Nature (London)* **197**, 755 (1963).
19. B. Belbeoch, J. C. Boivineau, and P. Perio, *J. Phys. Chem. Solids* **28**, 1267 (1967).
20. W. L. Roth, *Acta Crystallogr.* **13**, 140 (1960).
21. J. Manenc, J. Bougeot, and J. Benard, *C. R. Acad. Sci. Paris* **256**, 931 (1963).
22. F. Koch and J. B. Cohen, *Acta Crystallogr.* **B25**, 275 (1969).